

Chemisorption of C₂₈ fullerene on *c*(4×4) reconstructed GaAs(001) surface: A density functional theory study

Shujuan Yao,^{1,2} Chenggang Zhou,^{1,2} Liancai Ning,^{1,2} Jinping Wu,^{1,2} Zhenbang Pi,^{1,2} Hansong Cheng,¹ and Yuansheng Jiang³

¹*Institute of Theoretical Chemistry and Computational Materials Science, China University of Geosciences, Wuhan 430074, China*

²*Faculty of Materials Science and Chemical Engineering, China University of Geosciences, Wuhan 430074, China*

³*Institute of Theoretical and Computational Chemistry, Nanjing University, Nanjing 210093, China*

(Received 5 November 2004; published 17 May 2005)

Chemisorption of fullerenes on semiconductor surfaces is of current technological interest. Using *ab initio* density functional theory under the generalized gradient approximation, we performed extensive theoretical studies on the chemisorption of a small fullerene molecule, C₂₈, on the *c*(4×4) reconstructed GaAs(001) surface. The chemisorption structures and energetics at various adsorption sites, in combination of possible fullerene configurations, were carefully examined and the adsorption at the trench site with one hexagon of C₂₈ facing down was found to be energetically most favorable. In all cases, we found that upon C₂₈ adsorption the *c*(4×4) reconstructed GaAs(001) surface undergoes considerable lattice relaxation and structural deformation of fullerene molecule also occurs. The chemisorption is dictated by the [2+2] cycloaddition reaction and/or by simple electron lone pair mediated charge transfer reaction from the substrate to the fullerene molecule. It was found that the monolayer formed by the C₂₈ molecules on the surface is stable and naturally porous.

DOI: 10.1103/PhysRevB.71.195316

PACS number(s): 68.47.Fg

I. INTRODUCTION

There have been intensive experimental and theoretical efforts in recent years to develop novel semiconductor materials as the microelectronics industry evolves into ultralarge-scale integration.^{1,2} The design of materials with the desired physical properties, such as a low dielectric constant (low-*k*),³⁻⁵ to form thin films on semiconductor surfaces is one of the focal points and has presented a great challenge to the material community. GaAs represents one of the most important semiconductor materials and has been widely used for a broad variety of applications in microelectronics.^{6,7} As the size of semiconductor chips continues to shrink, increasingly new applications can be found by developing novel chemistries on the semiconductor surfaces. For instance, there is an increasing demand for a lower value of dielectric constant materials and a higher stability of the low-*k* films. One of the important requirements on the low-*k* materials is the high porosity.³⁻⁸ There have been intensive research activities in the past few years to deposit well-ordered films of organic precursors containing π bonds on semiconductor surfaces via a cycloaddition process.⁹⁻¹⁷ Much of the effort has centered around developing a novel chemistry on silicon surfaces¹³⁻¹⁵ and, to a much lesser extent, on GaAs surfaces.¹⁸⁻²⁰ The organic films so deposited can be very stable due to the formation of strong chemical bonds and well-ordered structures since the surface chemistry is highly bond selective, but the microporosity may still be an issue of concern. Recently, there have been several reports on depositing fullerenes on semiconductor surfaces.²¹⁻²⁵ Fullerenes are made of pentagons and hexagons of carbons containing alternative double bonds. In principle, they may also undergo the cycloaddition reactions similar to the organic precursors. Nevertheless, the chemical process may be more complex since several π bonds of fullerenes may participate the surface reactions simultaneously, depending on the adsorption sites and the elec-

tron delocalization. The fullerene-based precursors may be potentially useful to serve as low-*k* materials or surface passivation agents due to their high volumes with ample space inside the spheres and their strong chemical bonding with the semiconductor surfaces. Since the dielectric constant decreases as the porosity of the film increases, one may be able to effectively control the dielectric properties of the films by carefully selecting the appropriate size of fullerenes for deposition. Several experimental studies have demonstrated that the adsorption of fullerenes on semiconductor surfaces, such as Si(100) and GaAs(100), are highly stable and genuine chemical bonds between fullerenes and the substrates can be formed.²⁶⁻²⁸ However, to date, detailed adsorption structures and bond strength for fullerenes on GaAs surfaces have not been reported, perhaps partly due to lack of theoretical studies on the electronic structures.

In this paper, we present the first-principles based computational studies on C₂₈ adsorption at GaAs(001) surface using *ab initio* density functional theory. C₂₈ is one of the smallest fullerenes and is composed of 12 pentagons and 4 hexagons with a *T_d* symmetry.²⁹ Each side of the hexagon connects with a pentagon.^{30,31} The C-C-C angle in C₂₈ ranges from 107.8 deg to 110.6 deg, very close to a typical *sp*³ carbon, which imposes exceedingly high strains on the bonds. As a consequence, the π -orbital overlap is extremely deficient, leading to weak π bonds and thus poorly saturated carbons. As a consequence, these π bonds should be much easier to break. Therefore, small fullerenes like C₂₈ are expected to exhibit a higher reactivity compared with C₆₀ or other smaller curvature graphitic carbons. GaAs(001) is one of the most well-studied semiconductor surfaces due to its technological importance.³²⁻³⁴ It undergoes substantial reconstructions and exhibits a variety of well-ordered phases under different preparation conditions.³⁵⁻³⁸ In the present study, we selected an arsenic-rich phase *c*(4×4) reconstructed GaAs(001) surface as the substrate. The surface can be ob-

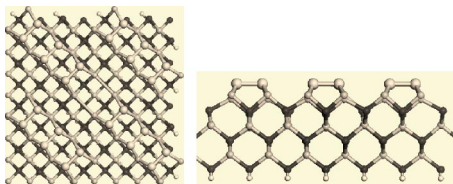


FIG. 1. The structure of the GaAs(001) $c(4 \times 4)$ reconstructed surface. The top view of the 2×2 unit cell illustrates the surface arrangement of the three-dimer units. The side view is along the direction of $[110]$. The white balls represent the As atoms and the black balls denote the Ga atoms. The top layer As dimers are highlighted with large balls.

tained upon annealing to room temperature and has been shown to be very stable.^{36,37} The electronic structure of the $c(4 \times 4)$ surface was studied in detail by Strasser and co-workers.^{39,40} The top layer is covered by three arsenic dimers along the $[110]$ direction, as shown in Fig. 1; each atom of the dimer connects with the top arsenic layer with two bonds and with another atom of the dimer via a single bond, leaving an electron lone pair on its p orbital. This unique structural arrangement provides the $c(4 \times 4)$ surface with several possible adsorption sites for C_{28} , which include (1) the site on a single dimer; (2) the site on top of two adjacent dimers of the three-dimer unit noted as the double-dimer site; and (3) the large trenches between two nearest neighboring three-dimer units. In addition, the orientation of C_{28} will also influence the adsorption patterns. We thus expect that the small fullerene molecule will interact with the surface substrate via a variety of mechanisms. In the present computational studies, we will systematically examine all the above adsorption patterns and possible sites. Our primary objective is to understand the nature of the C_{28} adsorption on the GaAs(001) surface and to predict the chemical/physical properties of the fullerene film on the surface through the first-principles quantum-mechanical calculations. We show that C_{28} can form a variety of adsorption patterns on the $c(4 \times 4)$ reconstructed GaAs(001) surface with strong bonding. This novel surface chemistry may lead to the development of well-controlled fullerene films with desired porosity, thickness, and strength.

II. COMPUTATIONAL DETAILS

All calculations were performed using *ab initio* density functional theory under the generalized gradient approximation as proposed by Perdew-Wang^{41–44} and implemented in the SIESTA simulation code.^{45–49} Norm-conserving pseudopotentials were used to replace the core electrons and the strictly localized numerical atomic orbitals of double- ζ plus polarization function quality as the basis set were employed to describe the valence electrons. A cutoff energy of 200 Ry yielded results with good accuracy. A periodic boundary condition was imposed on a slab model of the GaAs(001) $c(4 \times 4)$ surface. The Brillouin zone integration was performed using a special k -point approach, as implemented with the Monkhorst and Pack scheme with $2 \times 2 \times 1$ k points. The present computational method has been widely utilized in a

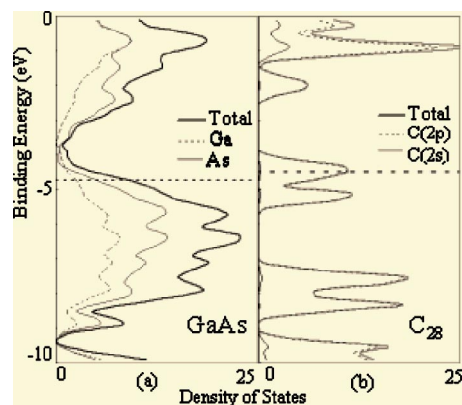


FIG. 2. The calculated density of states (DOS): (a) DOS of the GaAs substrate; (b) DOS of C_{28} in the gas phase.

broad variety of surface chemistry studies and shown to be highly accurate in providing reliable information on surface structures and energetics.^{45,50}

The primitive unit cell contains seven layers of GaAs alternated with a gallium layer and an arsenic layer, respectively. But the top two layers are constituted only by As atoms and the bottom Ga layer is saturated with hydrogen atoms (Fig. 1). The surface cell parameters were taken from the crystal structure of GaAs and the distance between adjacent slabs was chosen to be 27 \AA , large enough to prevent effective interaction between slabs. The unit cell contains 24 Ga atoms, 30 As atoms, and 16 H atoms in addition to a C_{28} molecule. The closest distance between two nearest neighboring C_{28} molecules is approximately 6 \AA and thus the lateral interaction is very small. We performed full structural optimization for the top five layers of the surface together with the adsorbate and kept the bottom two layers as well as the hydrogen atoms fixed using the conjugate gradient algorithm without symmetry constraints. The adsorption energy of the fullerene is calculated using Eq. (1),

$$\Delta E_{\text{ads}} = E(\text{sub}_{\text{GaAs}} + C_{28}) - E(\text{sub}_{\text{GaAs}}) - E(C_{28}), \quad (1)$$

where $E(\text{sub}_{\text{GaAs}} + C_{28})$, $E(\text{sub}_{\text{GaAs}})$, and $E(C_{28})$ represent the total energies of the $c(4 \times 4)$ reconstructed GaAs(001) surface with an adsorbate, the surface itself, and C_{28} , respectively.

III. RESULTS AND DISCUSSION

We first performed energy minimization for the GaAs(001) $c(4 \times 4)$ surface. The optimized structure is shown in Fig. 1. The bond distance of the As dimer in the top layer is 2.609 \AA for the mid-dimer and 2.636 \AA for the dimers on the two sides. The distance between the top layer As and the second layer As is 1.23 \AA . The short distances reflect the quasistable nature of the dangling bonds of the As dimers. Figure 2(a) shows the calculated density of states (DOS) of the GaAs(001) $c(4 \times 4)$ surface. The calculated band gap is about -1.6 eV , slightly larger than that of the bulk, which is -1.42 eV . Both the valence band and the conduction band are essentially dominated by the contribution from the As atoms, especially the As dimers. For comparison

purposes, we display the calculated density of states of gas phase C₂₈ in Fig. 2(b).

The C₂₈ adsorption on the GaAs(001) $c(4 \times 4)$ surface may exhibit a variety of geometric patterns. The structure and strength are determined by both the surface adsorption sites and the orientation of the molecule. To facilitate the description of the adsorption structure, we first denote the surface single-dimer site, double-dimer site and the trench site with S, D, and T and use $\alpha, \beta, \gamma, \delta$ to represent, in the C₂₈ molecule, a single pentagon, a hexagon, a shared double bond of the adjacent pentagon and hexagon, and a shared double bond of the adjacent two hexagons, respectively. In the following, we will examine the C₂₈ adsorption at the three adsorption sites, as outlined above.

A. Single-dimer site

We first orient the C₂₈ molecule toward a top layer single As dimer with the $\alpha, \beta, \gamma, \delta$ orientations, respectively, followed by energy minimization of the structures. In most cases, cycloaddition reactions take place and strong covalent bonds are formed. Substantial molecular structural and lattice relaxations occur. The optimized structures with a top view and a side view are shown in Fig. 3 and the calculated spectra of density of states are shown in Fig. 4. The calculated adsorption energies are shown in Table I.

For S^α , the structural optimization results in the fullerene molecule falling into the double-dimer site. Four covalent bonds between C₂₈ and two arsenic dimers of the top layer are formed; three of the new bonds are with bond distances ranging from 2.126 Å to 2.147 Å and the fourth one is relatively weak with a bond length of 2.884 Å, reflecting the geometric incommensurability. The arsenic dimer bond distances are subsequently elongated by 0.025 Å upon C₂₈ adsorption. Likewise, the bond distances of the four carbon atoms participating in the surface reaction are also increased slightly compared with their gas-phase values. Part of the fullerene structure near the adsorption site becomes considerably deformed as the molecule forms new bonds with the surface. The adsorption also makes a considerable impact on the top layer structure as the interlayer distance near the binding site between the arsenic layers is changed from 1.23 Å to 1.27 Å and the distance between the second As layer and the top Ga layer is increased from 1.25 Å to 1.29 Å [Fig. 3(a)].

The attachment of C₂₈ at the surface is dictated by two of the so-called [2+2] cycloaddition reactions. The highly unsaturated As dimer is reacting with the unoccupied π orbitals of C₂₈, forming a four-membered ring with two new σ bonds between As and C atoms. The double-dimer site allows two As dimers and a diene segment of the pentagon in C₂₈ to participate in the cycloaddition reactions simultaneously. However, one of the two cycloaddition reactions is incomplete due to the structural incommensurability. Mulliken population analysis indicates that charge transfer from an arsenic dimer to C₂₈ by a 0.333 electron. The reaction gives rise to an adsorption energy of -1.88 eV, suggesting that the adsorption structure is highly stable at this site. Figure 4(a) displays the calculated density of states spectrum. Compared with the DOS spectrum of the substrate [Fig. 2(a)], the va-

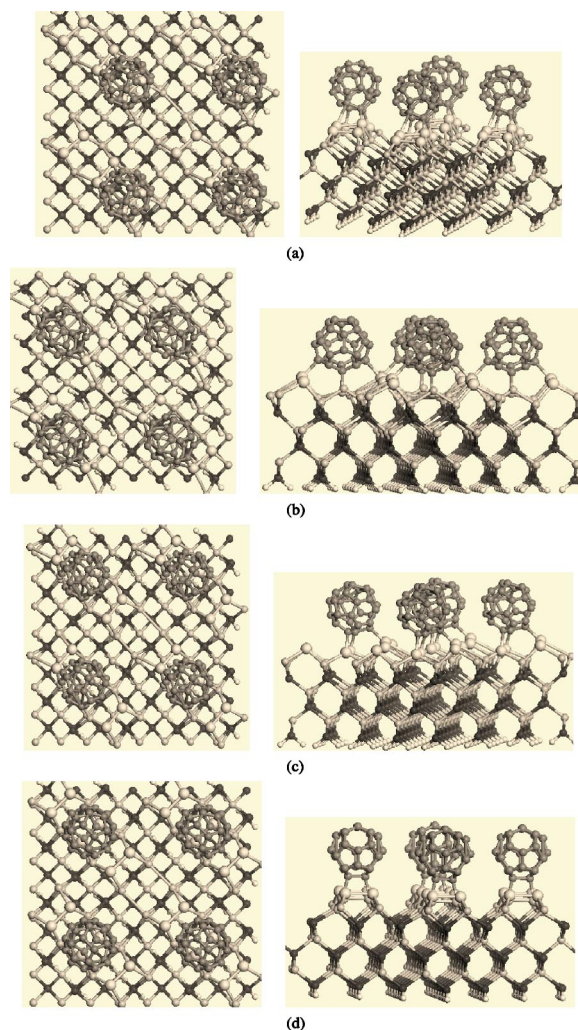


FIG. 3. The optimized structure of C₂₈ on the GaAs(001) $c(4 \times 4)$ reconstructed surface with a top view and a side view along the [110] direction. (a) S^α : the pentagon of C₂₈ facing down along the single dimer. (b) S^β : the hexagon of C₂₈ facing down the single-dimer. (c) S^γ : a shared double bond of the adjacent pentagon and hexagon in C₂₈ facing down. (d) S^δ : a shared double bond of the adjacent two hexagons in C₂₈ facing down.

lence band of the S^α system is broadened slightly across the Fermi level. Much of the contribution comes from the conduction band of C₂₈, which consists of mostly the antibond-

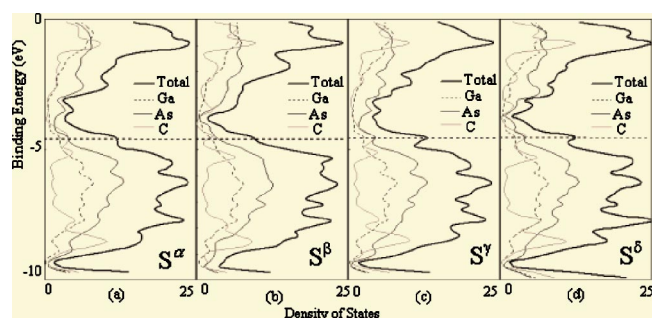


FIG. 4. The calculated density of states (DOS): (a) S^α , (b) S^β , (c) S^γ , and (d) S^δ .

TABLE I. The calculated adsorption energies of C_{28} at the single-dimer (S), double-dimer (D) and trench (T) sites of GaAs(001) surface with various conformations and the corresponding Mulliken charges transferred from the surface to C_{28} .

Site	Orientation	Adsorption energy (eV)	Charge transfer
Single	S^α	-1.88	0.333
	S^β	-1.63	0.34
	S^γ	-1.33	0.361
	S^δ	-1.33	0.216
Double	D^α	-2.16	0.296
	D^β	-1.95	0.244
Trench	T^α	-2.21	0.318
	T^β	-3.02	0.359

ing π orbitals. The DOS spectrum indicates that the overlap between the valence band of the substrate, which is governed primarily by the unsaturated orbitals of As dimers, and the conduction band of C_{28} gives rise to the strong chemisorption, allowing C_{28} to accept electrons from the surface. The change in the valence band and the conduction band is largely dictated by the As dimers and C_{28} and a small contribution comes from the rest of the GaAs layers.

For S^β , the fullerene was placed on top of the middle As dimer with a hexagon facing down with the anticipation that a $[2+4]$ cycloaddition reaction might occur. However, energy minimization results in a quite unexpected chemisorption structure: the fullerene molecule inclines to lean to the trench site slightly; the two adjacent pentagons are then reacting with the end atoms of the three As dimers by forming three new covalent bonds, creating two adjacent six-membered ring structures [Fig. 3(b)] with a chair conformation. The distance of the C-As σ bond in the middle is 1.988 Å, while the bond length of the other two on the sides is 2.208 Å. The As dimer loosens up with the bond length increased lightly from 2.636 Å to 2.656 Å. The two side As dimers bonding with C_{28} tilts up toward the adsorbate and the As dimer in the middle is pushed downward slightly. Considerable relaxation between the top Ga layer and the second As layer upon C_{28} adsorption is observed as the interlayer distance is increased from 1.24 Å to 1.32 Å. Structural deformation of the fullerene is also noted here as the two pentagons form new chemical bonds with the surface. The calculated adsorption energy is -1.63 eV, indicating that C_{28} is stable at this site.

The chemisorption is governed by the charge transfer from the electron lone pairs of the As dimers to the empty π bands of C_{28} with about 0.34 electrons being transferred. Indeed, the calculated DOS spectrum [Fig. 4(b)] indicates that the empty π bands of C_{28} and the low lying states of the dimers make most of the contributions to the conduction band near the Fermi level, supporting the charge transfer mechanism. A detailed analysis suggests that feature changes observed in the DOS spectrum are attributed mainly to the two top layers of As atoms and C_{28} and the electronic structure of the inner layer atoms remain essentially intact.

Next, we examine the S^γ configuration by aiming the double bond shared by a pentagon and a neighboring hexagon in C_{28} at the single-dimer site. As expected, the $[2+2]$ cycloaddition reaction takes place to form a four-membered ring structure with the bond distances of the two new σ bonds being 2.137 Å and 2.141 Å, respectively [Fig. 3(c)]. However, this configuration is not stable as the standing new ring structure does not adequately support the adsorbate. As a consequence, the fullerene is twisted slightly to form an additional σ bond with the end atom of a neighboring As dimer with a bond length of 2.128 Å. Compared with S^α and S^β , this chemisorption structure is much less stable. The calculated adsorption energy is only -1.33 eV. Like the above two cases, charge transfer from the substrate to the fullerene molecule by 0.361 electrons provides the driving force for the surface reaction. The calculated DOS spectrum [Fig. 4(c)] indeed indicates that the empty π bands of C_{28} and the electron lone pairs of the As dimers dominates the valence band, consistent with the charge transfer mechanism described in the above.

Finally, we lined up a double bond shared by two adjacent pentagons with the As dimer in the middle and then performed the energy minimization (S^δ). A typical $[2+2]$ cycloaddition reaction takes place with two σ bonds between carbon atoms and arsenic atoms formed in a four-membered ring structure. The optimized structure, shown in Fig. 4(d), is symmetric with the two bond distances of 2.134 Å, and 2.137 Å, respectively. This structure is not expected to be very stable since the standing four-ring adsorption structure is very sloppy and can hardly support the fullerene. This is confirmed by the smaller calculated adsorption energy, -1.33 eV. The calculated DOS spectrum displayed in Fig. 4(d) can be interpreted in the same fashion as in S^γ .

It is clear that at the single-dimer site, the most stable adsorption configuration is S^α . The chemisorption process takes advantage of two cycloaddition reactions to support the adhesion of fullerene on the $c(4 \times 4)$ reconstructed GaAs(001) surface. Nevertheless, due to the initial structural alignment prior to the energy minimization, these reactions result in only three strong covalent bonds. It is thus expected that with careful alignment of the initial configuration of C_{28} toward the As dimers, it is possible to achieve higher adsorption energies at the double-dimer site.

B. Double-dimer site

We examined two configurations of C_{28} at the double-dimer site: one with a pentagon lining up with two As dimer bonds (D^α) and another with a hexagon facing the dimers (D^β). The optimized structures with a top view and a side view are shown in Fig. 5 and the simulated spectra of the density of states are displayed in Fig. 6. The calculated adsorption energies of the two configurations at this site are shown in Table I.

For D^α , the optimized chemisorption structure shown in Fig. 5(a) is somewhat similar to the one for S^α [Fig. 3(a)] although the detailed geometric arrangement differs. Like S^α , two $[2+2]$ cycloaddition reactions occur; one is complete and another is not due to the incommensurability between the pentagon and the two As dimers. As a consequence, only

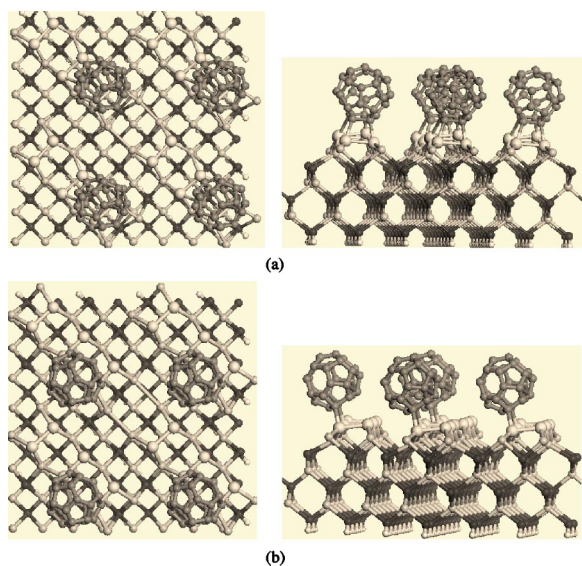


FIG. 5. The optimized structure of C₂₈ on the GaAs(001) $c(4 \times 4)$ reconstructed surface with a top view and a side view along the [110] direction. (a) D^α : a pentagon of C₂₈ facing down the double-dimer unit. (b) D^β : a hexagon face down the double-dimer unit.

three genuine σ bonds are formed with bond distances of 2.162 Å, 2.184 Å, and 2.117 Å, respectively. The incomplete cycloaddition yields a weak bond with a bond length of 3.134 Å. However, unlike S^α , the C=C bond of C₂₈ participating in the complete cycloaddition is from the shared bond between two adjacent pentagons instead of being between a pentagon and a hexagon, as is the case for S^α . Therefore, the geometry is less strained. Indeed, the C—C bond is stretched more significantly upon C₂₈ adsorption than in the case of S^α (from 1.452 Å to 1.626 Å in D^α versus from 1.448 Å to 1.593 Å in S^α). The calculated adsorption energy is -2.16 eV, slightly higher than the one in S^α . The Mulliken population analysis gives a charge transfer of 0.296 electrons from the substrate to the fullerene. The lattice relaxation occurs mainly near the adsorption site. The DOS spectrum shown in Fig. 4(a) exhibits similar features as in the case of S^α .

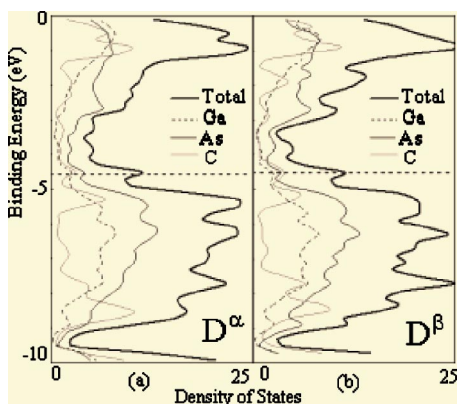


FIG. 6. The calculated density of states (DOS): (a) D^α and (b) D^β .

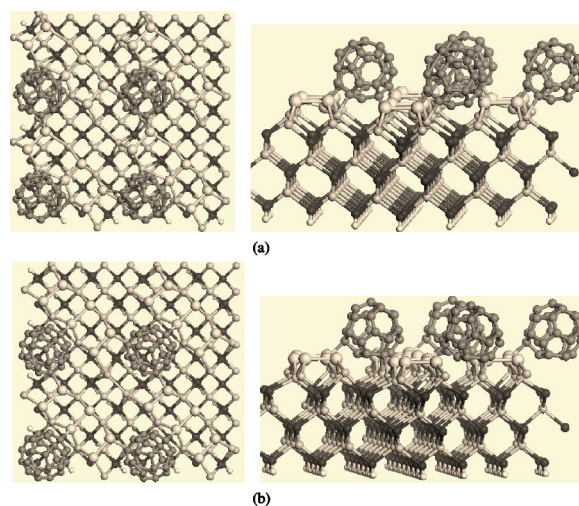


FIG. 7. The optimized structure of C₂₈ on the GaAs(001) $c(4 \times 4)$ reconstructed surface with a top view and a side view along the [110] direction. (a) T^α : the pentagon of C₂₈ facing down the trench site. (b) T^β : the hexagon of C₂₈ facing down the trench site.

Surprisingly, a perfectly well-aligned initial structure with two parallel C=C bonds of a hexagon in C₂₈ aligned with two As dimers (D^β) did not lead to two [2+2] cycloaddition reactions upon energy minimization. Instead, the two end atoms of the C=C bonds interact directly with the nearby end atoms of the adjacent As dimers to form two C—As σ bonds with the bond distances of 2.147 Å and 2.088 Å, respectively. The adsorption yields a six-membered ring structure with a “boat” conformation. The adsorbate tilts slightly toward the trench site, as shown in Fig. 3(b). The calculated adsorption energy is -1.95 eV, suggesting that this is a stable adsorption site. Once again, the chemisorption is governed by the charge transfer (0.244 electrons) from the As dimers to the empty π bands of fullerene, as is clearly shown by the calculated DOS spectrum.

In general, the chemisorption of C₂₈ at the double-dimer site is energetically more favorable. The fullerene molecule is well supported by the As dimers via the formation of C—As σ bonds.

C. Trench site

The trench site is the confined area of the surface surrounded by four three-dimer units as shown in Fig. 1. It is about 8 Å wide and 13 Å long. Unlike the As atoms right underneath the dimers, each of the four As atoms inside the trench area connects with a dimer atom and two Ga atoms in the next layer, leaving one dangling bond. We thus expect that these atoms are also chemically active besides the highly unsaturated dimer bonds.

We place C₂₈ on the trench site with a pentagon (T^α) and a hexagon (T^β) oriented toward the surface, respectively. The optimized structures with a top view and a side view are displayed in Fig. 7 and the calculated spectra of density of states are shown in Fig. 8. A detailed examination of these structures indicates that C₂₈ forms strong covalent bonds with the $c(4 \times 4)$ reconstructed surface.

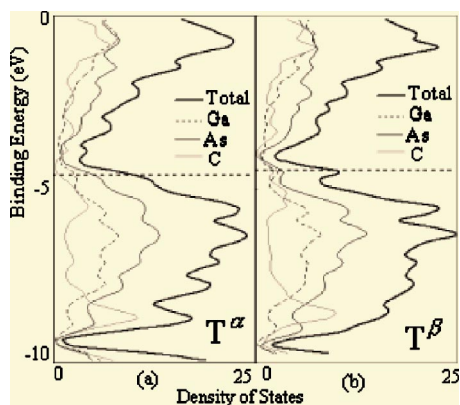


FIG. 8. The calculated density of states (DOS): (a) T^α and (b) T^β .

For C_{28} with the pentagon facing down (T^α), there are four covalent bonds formed with the substrate. The calculated bond lengths range from 2.091 Å to 2.201 Å. The fullerene molecule interacts with the end atoms of three neighboring As dimers and one atom of the second As layer [Fig. 7(a)], forming new σ bonds. Substantial structural relaxation takes place. First, C_{28} is now partially embedded in the trench site. Consequently, the surface As dimers are slightly reorganized; the dimer closer to the adsorbate is “squeezed” slightly by C_{28} in the trench, making a shorter bond length of 2.542 Å, while the bond distances of the other dimers become elongated to 2.704 Å since one of the end atoms are pulled over toward the fullerene. Second, the chemisorption also results in considerable lattice relaxation as both the second layer As atoms and the top layer Ga atoms shift their positions from their original equilibrium locations; those close to the adsorbate are pulled up and others adjust their positions accordingly, leading to a slight misalignment of the top few layers. Consequently, the calculated adsorption energy, which is -2.21 eV, is significantly enhanced. Mulliken population analysis suggests that 0.318 electrons are transferred from the substrate to the fullerene molecule. Figure 8(a) displays the calculated density of states. Compared with the DOS spectrum of the substrate, the spectrum is broadened, reflecting the top layer structural change.

Finally, we examine the adsorption of C_{28} on the surface with a hexagon oriented to the trench site (T^β). The optimized structure is shown in Fig. 7(b). The atoms on the hexagon essentially reside at the same layer of the As dimers. Three distinct σ bonds between C_{28} and the surface are formed with bond distances of 2.071 Å, 2.071 Å, and 2.201 Å, respectively; two bonds are created via interaction between C_{28} and two atoms in the second As layer and the third one is between an atom in the hexagon of C_{28} and the end atom of the As dimer in the middle of the three-dimer unit. The dimer participated in the bond formation is stretched significantly from 2.609 Å to 2.792 Å. This structural arrangement seems to fit the trench site extremely well. All atoms on the hexagon are within 3.6 Å away from the nearby surface atoms to maximize the interactions. Compared with the T^α configuration, this structure appears to cause less structural rearrangement in the lattice and is more stable. Indeed, the calculated adsorption energy, -3.02 eV,

yields the highest strength at this site among all the adsorption sites we have investigated. The stronger chemisorption arises from the higher charge transfer (0.359 electrons) from the surface to the C_{28} . The dangling bonds of As atoms at the trench site as well as the As dimer provide the major driving force for the adsorption. The calculated DOS spectrum [Fig. 8(b)] has a distinct feature around the Fermi level contributed mostly by the As dimer p orbitals and the empty π orbitals of C_{28} .

IV. SUMMARY

We have conducted an extensive computational study using density functional theory on the chemisorption of a small fullerene molecule, C_{28} , on the $c(4 \times 4)$ reconstructed GaAs(001) surface. Adsorption at various adsorption sites coupled with several possible orientations of the fullerene molecule was carefully examined. In all cases, we found that the adhesion of C_{28} on the surface is strong and chemically stable covalent bonds between the fullerene and the substrate are formed. The chemisorption results in lattice relaxation and structural distortion of the fullerene molecule to a certain extent, depending on the adsorption site and fullerene orientation. It was found that the strongest chemisorption takes place at the trench site with a hexagon of C_{28} facing down the surface and the weakest adsorption occurs at the single-dimer site.

The dominant force for the chemisorption is the interaction between the empty π bands of fullerene, which acts as an electron acceptor, and the electron lone pairs of the p orbitals of As, which behaves as an electron donor. The electron lone pairs reside not only on the As dimers but also on the As atoms confined in the trench area. They allow the surface to undergo either a $[2+2]$ cycloaddition reaction or simple charge transfer reactions with the incoming adsorbate with unsaturated bonds. These reactions are competing with each other and the optimal adsorption configuration is highly dependent on the geometric arrangement that gives rise to the maximum bonding. Our results suggest that the $[2+2]$ may not be the only driving force for the chemisorption of C_{28} on the GaAs(001) surface, a feature that is strikingly different from most of the small organic molecules with unsaturated bonds on silicon surfaces, where the cycloaddition reaction dominates the surface reaction. Instead, the dangling bonds at the trench site can mediate the chemisorption in conjunction with the unsaturated dimer bonds. For the present system, we found that this arrangement gives the highest adsorption energy. Finally, in all cases, no $[4+2]$ cycloaddition reaction was found to occur. The results presented in this paper suggest that the adsorption of C_{28} on the $c(4 \times 4)$ reconstructed GaAs(001) surface can be stable and the monolayer is highly porous.

ACKNOWLEDGMENTS

We would like to thank Dr. W. G. Schmidt for sending us the structure of the $c(4 \times 4)$ reconstructed GaAs(001) surface. Support from China University of Geosciences is gratefully acknowledged.

- ¹M. Bohr, IEEE IEDM Tech. Dig. 241, 1995.
- ²W. W. Lee and P. S. Ho, MRS Bull. **22**(10), 19 (1997).
- ³G. Ruan and X. Xiao, Acta Electron. Sin. **28**, 84 (2000).
- ⁴L. Peters, Semicond. Int. **21**, 64 (1998).
- ⁵R. Sharang pani and R. Sing, Rev. Sci. Instrum. **68**, 1564 (1997).
- ⁶J. S. Blakemore, J. Appl. Phys. **53**, 123 (1982).
- ⁷S. Adachi, J. Appl. Phys. **58**, 1 (1985).
- ⁸E. Korczynski, Solid State Technol. **42**, 43 (1999).
- ⁹R. Konečný and D. J. Doren, Surf. Sci. **417**, 169 (1998).
- ¹⁰H. N. Waltenburg and J. T. Yates, Chem. Rev. (Washington, D.C.) **95**, 1589 (1995).
- ¹¹S. F. Bent, J. Phys. Chem. B **106**, 2830 (2002).
- ¹²R. J. Hamers, S. K. Coulter, M. D. Ellison, J. S. Hovis, D. F. Padowitz, M. P. Schwartz, C. M. Greenlief, and J. N. Russell, Jr., Acc. Chem. Res. **33**, 617 (2000).
- ¹³R. Konečný and D. J. Doren, J. Am. Chem. Soc. **119**, 11098 (1997).
- ¹⁴R. J. Hamers, J. S. Hovis, S. Lee, H. Liu, and J. Shan, J. Phys. Chem. B **101**, 1489 (1997).
- ¹⁵M. R. Linford, P. Fenter, P. M. Eisenberger, and C. E. D. Chidsey, J. Am. Chem. Soc. **117**, 3145 (1995).
- ¹⁶Y. Cui, Q. Wei, H. Park, and C. M. Lieber, Science **293**, 1289 (2001).
- ¹⁷F. J. Meyer zu Heringdorf, M. C. Reuter, and R. M. Tromp, Nature (London) **412**, 517 (2001).
- ¹⁸R. A. Wolkow, Annu. Rev. Phys. Chem. **50**, 413 (1999).
- ¹⁹G. P. Lopinski, T. Fortier, D. J. Moffatt, and R. A. Wolkow, J. Vac. Sci. Technol. A **16**, 1037 (1998).
- ²⁰S. Gokhale, P. Trischberger, D. Menzel, W. Widdra, H. Dröge, H. P. Steinrück, U. Birkenheuer, U. Gutdeutsch, and N. Rösch, J. Chem. Phys. **108**, 5554 (1998).
- ²¹R. Notzel, J. Temmyo, and T. Tamamura, Appl. Phys. Lett. **64**, 3557 (1994).
- ²²M. Pristovsek, H. Menhal, J. T. Zettler, T. Schmidling, N. Esser, W. Richter, C. Setzer, J. Platen, and K. Jacobi, J. Cryst. Growth **195**, 1 (1998).
- ²³D. Kisker, G. Stephenson, I. Kamiya, P. Fuoss, D. Aspnes, L. Mantese, and S. Brennan, Phys. Status Solidi A **152**, 9 (1995).
- ²⁴W. Kratshmer, L. D. Lamb, K. Fostiropovios, and D. R. Huffman, Nature (London) **85**, 354 (1990).
- ²⁵T. Sakurai, X. D. Wang, O. K. Xue, Y. Hasegawa, T. Hashizume, and H. Shinohara, Surf. Sci. **51**, 263 (1996).
- ²⁶M. D. Pashley, K. W. Haberern, W. Friday, J. M. Woodall, and P. D. Kirchner, Phys. Rev. Lett. **60**, 2176 (1988).
- ²⁷T. Hashizume, Q. K. Xie, J. Zhou, A. Ichimiya, and T. Sakurai, Phys. Rev. Lett. **73**, 2208 (1994).
- ²⁸J. E. Northrup and S. Froyen, Phys. Rev. B **50**, 2015 (1994).
- ²⁹S. Zhong and C. Liu, J. Mol. Struct.: THEOCHEM **392**, 125 (1997).
- ³⁰M. H. Lin, Y. N. Chiu, S. T. Lai, J. M. Xiao, and M. Z. Fu, Fullerene Sci. Technol. **5**(1), 111 (1997).
- ³¹J. M. Xiao, M. H. Lin, Y. N. Chiu, M. Z. Fu, S. T. Lai, and N. N. Li, J. Mol. Struct.: THEOCHEM **428**, 149 (1998).
- ³²M. L. Yu and L. A. Delouise, Surf. Sci. Rep. **19**, 285 (1994).
- ³³J. F. Whitaker, Mater. Sci. Eng., B **22**, 61 (1993).
- ³⁴J. Herfort, G. Apostolopoulos, K. J. Friedland, H. Kostial, W. Ulrici, L. D. Aweritz, M. Leitner, P. Glas, and K. H. Ploog, Jpn. J. Appl. Phys., Part 1 **39**, 2452 (2000).
- ³⁵M. Ozeki, Mater. Sci. Rep. **8**, 97 (1992).
- ³⁶Q. Chen, C. A. Beyler, P. D. Dapkus, J. J. Alwan, and J. J. Coleman, Appl. Phys. Lett. **60**, 2418 (1992).
- ³⁷C. H. Chen, C. A. Larsen, and G. B. Stringfellow, Appl. Phys. Lett. **50**, 218 (1987).
- ³⁸C. L. Larsen, N. I. Buchen, S. H. Li, and G. B. Stringfellow, J. Cryst. Growth **94**, 663 (1989).
- ³⁹I. Bartoš, T. Strasser, and W. Schattke, Prog. Surf. Sci. **74**, 293 (2003).
- ⁴⁰M. Steslicka, R. Kucharczyk, A. Akjouj, B. Djafari-Rouhani, L. Dobrzynski, and S. G. Davison, Surf. Sci. Rep. **47**, 93 (2002).
- ⁴¹J. P. Perdew, J. A. Chevary, S. H. Vosko, K. A. Jackson, M. R. Pederson, D. J. Singh, and C. Fiolhais, Phys. Rev. B **46**, 6671 (1992).
- ⁴²J. P. Perdew and Y. Wang, Phys. Rev. B **45**, 13244 (1992).
- ⁴³S. H. Vosko, L. Wilk, and M. Nusair, Can. J. Phys. **58**, 1200 (1980).
- ⁴⁴J. P. Perdew, K. Burke, and M. Ernzerhof, Phys. Rev. Lett. **77**, 3865 (1996).
- ⁴⁵J. M. Soler, E. Artacho, J. D. Gale, A. García, J. Junquera, P. Ordejón, and D. Sánchez-Portal, J. Phys.: Condens. Matter **14**, 2745 (2002).
- ⁴⁶S. K. Estreicher, K. Wells, P. A. Fedders, and P. Ordejón, J. Phys.: Condens. Matter **13**, 6271 (2001).
- ⁴⁷E. Artacho, D. Sánchez-Portal, P. Ordejón, A. García, and J. M. Soler, Phys. Status Solidi B **215**, 809 (1999).
- ⁴⁸D. Sánchez-Portal, P. Ordejón, E. Artacho, and J. M. Soler, Int. J. Quantum Chem. **65**, 453 (1997).
- ⁴⁹B. Caron and L. Derome *et al.*, Astropart. Phys. **10**, 369 (1999).
- ⁵⁰W. Kohn, Rev. Mod. Phys. **71**, 1253 (1999).